Journal of Bio- and Tribo-Corrosion (2024) 10:22
https://doi.org/10.1007/s40735-024-00822-8

Role of Thermal Spray Coatings on Erosion, Corrosion, and Oxidation in Various Applications: A Review

S. Suresh Kumar[1,2] · **C. Durga Prasad**[1,2] · **Harish Hanumanthappa**[1,2]

Received: 10 December 2023 / Revised: 28 December 2023 / Accepted: 10 January 2024 / Published online: 14 February 2024

Abstract
Depending on the location, extreme environmental conditions must have different graded properties. This is especially important for surfaces that are exposed to mechanical, chemical, thermal, and electrochemical interactions, as these can harm other components in use, such as gas turbines, ball valves, aerospace, power plants, and heat exchangers. The primary problems, such as oxidation, corrosion, erosion, and wear or their combinations will shorten the components life. One of the key deposition methods to address the said issues is thermal spray procedure. Amongst the several thermal spray approaches, the high-velocity oxy-fuel (HVOF) thermal spray technique is frequently used because of its improved performance, cheap expansion costs, and creation of high-density coatings with nominal porosity. In addition to discussing different coating materials and applications, this article provides an overview of advantages and limits of the HVOF spray method. This paper also addresses the impact of varying coating parameters on material significances relating to high-temperature performances, microstructural properties of HVOF spray technique, and electrochemical behaviours.

Keywords Thermal spray coatings · Corrosion · Oxidation · Hot corrosion · Erosion

1 Introduction

Engineering components require graded properties, affecting surfaces through frictional, thermal, mechanical, and chemical interactions. Monitoring Tribological and corrosion phenomena is crucial for recovery. India experiences an economy loss of $6500 US$ due to corrosion. Materials used in industrial applications must satisfy specific needs, such as strength and fracture resistance. The interaction between the environment and the material, particularly the surface, is critical [1–5]. Coatings have broadened design possibilities by combining bulk properties with surface capabilities. Examples include corrosion-resistant coatings for offshore structures and thermal barrier coatings (TBC) for turbine blades [6].

High-temperature-resistant materials and coatings are essential for power generation, shielding parts from oxidation and corrosion. Surface coating and alloy formation are strategies for mechanical strength in fossil fuel energy systems, with carbide-based cermets being popular due to their strength and stability [7–9]. Thermal spraying is a popular way for applying protective coatings and repairing large shafts in turbines and pumps, addressing metal degradation due to hot corrosion in high-temperature environments [10]. It is further classified as shown in Fig. 1 with features of various thermal spray methods as represented in Table 1. Whereas, HVOF coating is a prominent thermal spraying technique, using hydrogen and natural gases for controlled heat input [11–13]. One of the most prominent thermal spraying techniques is HVOF coating, which uses the combustion of hydrogen and natural gases or liquid fuel, producing high kinetic energy under controlled heat input [14]. The characteristics of various thermal spray methods are shown in Fig. 2a–d.

1.1 High-Velocity Oxy-Fuel (HVOF) Spray

HVOF is a thermal spray technology developed by Browning and Witfield in the 1980s using rocket engine technologies. It uses blend of oxygen and fuel gases to generate high temperatures and pressure, facilitating a supersonic gas flow

✉ C. Durga Prasad
durgaprasi71@gmail.com

1 Department of Mechanical Engineering, RV Institute of Technology and Management, Bengaluru 560076, India

2 Visvesvaraya Technological University, Belagavi, Karnataka, India

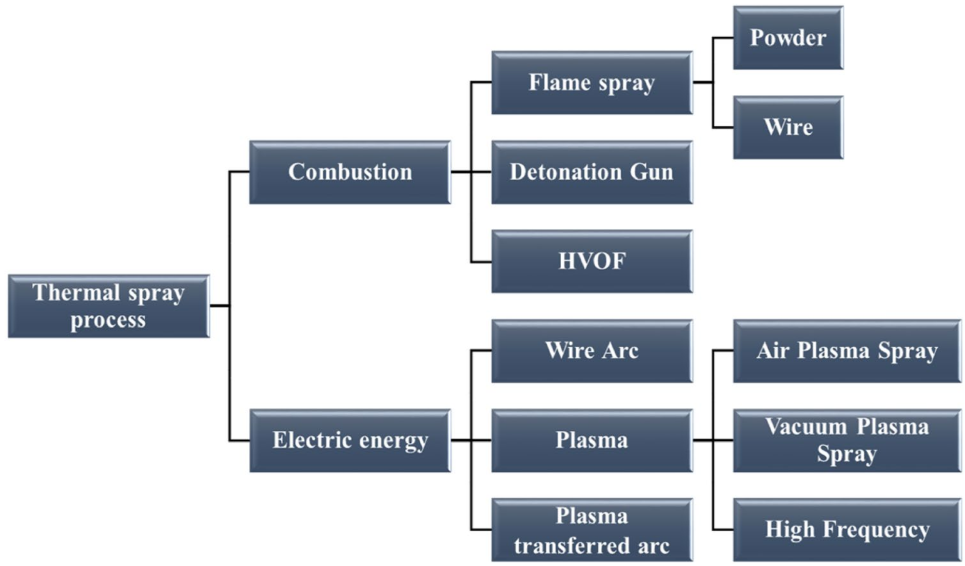

Fig. 1 Thermal spray process flowchart

Table 1 Features of various thermal spray methods [15, 97–102]

Deposition technique	Heat source	Material feed type	Coating materials	Spray Gun Temp. (°C)	Particle velocity (m/s)	Bond strength (MPa)	Porosity (% volume)	Hardness Rh scale Rc scale
Electric Arc	Arc between electrodes	Wire	Ductile	6000	240	40–60	8 to 15	40 35
Plasma Spraying	Plasma arc	Powder	Metallic ceramic compound	16,000	120–600	30–70	2 to 5	40 50
Flame Spraying	Oxyacetylene/ oxyhydrogen	Powder	Metallic ceramic	3300	240	20–28	10 to 20	30 20
Detonation Gun	Oxygen/acetylene/ nitrogen Gas detonation	Powder	Metallic ceramic compound	4500	800	> 70	0.1 to 1	**
Low Pressure Plasma	Plasma arc	Powder	Metallic ceramic compound	16,000	900	> 71	< 5	**
HVOF	Oxypropylene/ hydrogen/ Propane/LPG	Powder/ Wire	Metallic ceramic compound	2800	1350	40–96	< 1	100 50

**Not applicable

through nozzle. The process of spot melting is influenced by factors, such as flame temperature, dwell time, material melting point, and thermal conductivity [15–17]. HVOF differs from conventional flame spray using a supersonic jet, improving coating characteristics, especially for materials, like tungsten carbide coatings. The HVOF technique is a unique and alternative method of deposition, and optimum process parameters are evaluated for each composition [18]. The schematic representation of HVOF method is shown in Fig. 3.

HVOF process is thermal spray technique that uses high velocities to produce higher bond strength and lower porosity. HVOF offers advantages over other techniques, like uniform heating, shorter flight exposure time, lower surface oxidation, lower flame temperature, lower capital cost, and easier use. Additionally, it permits thicker coatings with increased density, impact energy, improved corrosion resistance, reduced porosity, hardness grades, improved bonding, and improved wear resistance. HVOF also offers smoother surfaces, thicker coatings, and shorter times at higher temperatures, and better chemical retention [19–22]. HVOF coating process involves setting up a machine according to manufacturer's instructions, with parameters clustered based on the coating material application. The coating process is influenced by input factors such as temperature, melting phase, and particle velocity [23]. The characteristics of

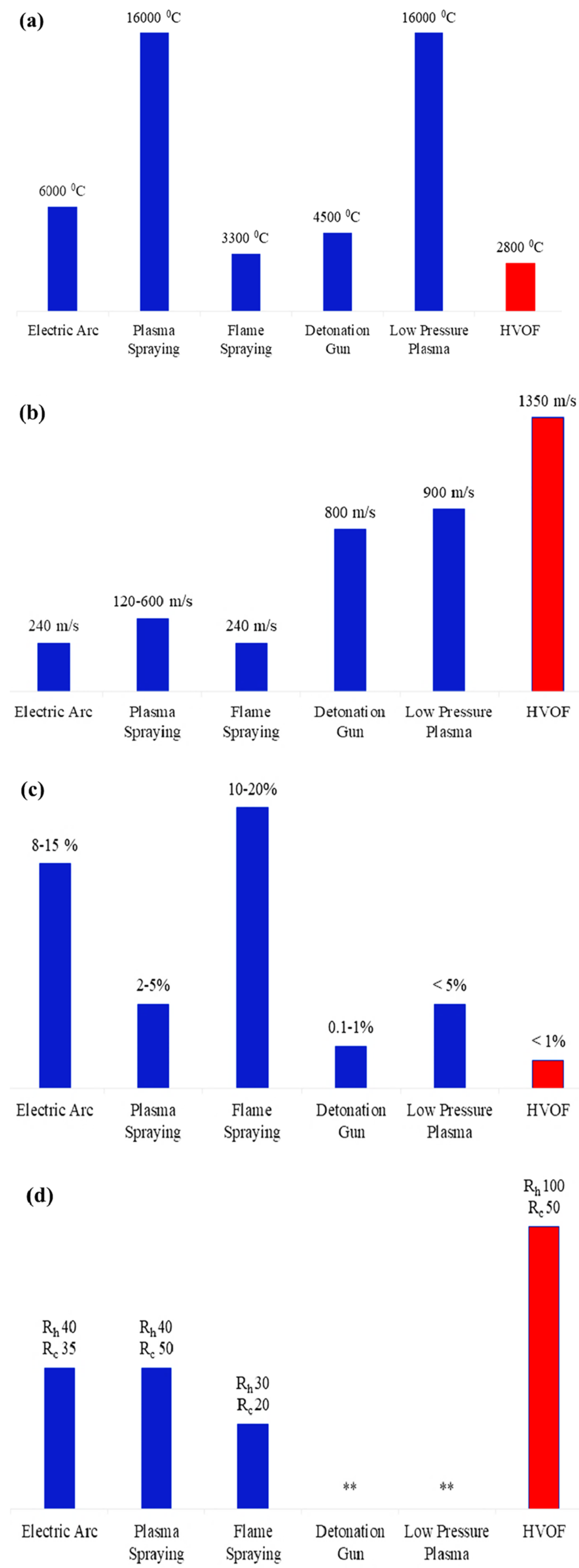

Fig. 2 Different thermal spray methods characteristics. **a** Spray gun temperature (°C), **b** Particle velocity (m/s), **c** Porosity volume (%), and **d** Hardness (Rh and Rc scale)

in-flight particles impact the adhesive strength and microstructure of coatings, with temperature and velocity having an impact on adhesive strength. Higher particle velocity reduces porosity and increases oxide content in the link between coating microstructure and particle in-flight characteristics [24].

1.2 Significance of HVOF Process Parameters

It was possible to create distinct coating layers with varying chemical compositions without stopping the spraying operation by modifying a conventional powder feed hopper to deposit two powders concurrently. In order to confirm that mixed composition particles are available, a process model was created to mimic the movement of nitrogen gas and powder. We built, commissioned, and calibrated a multi-powder feed device. Onto aluminium substrates, multi-layer coatings made of aluminium tool steel were sprayed [25–27].

To evaluate the coatings of the HVOF spraying technique, the learning used factorial design experiments. For combined coatings, the ideal set of spray parameters was similar to that for aluminium powder alone, maybe because of the powders' different temperatures. Altered types of composite coatings were placed using optimised spray parameters and coatings with thicker layers showed higher residual stress but improved hardness [27, 28].

The varying spray parameters of HVOF for various combinations of coatings to substrates are displayed in Table 2. Whereas, in spray process, standoff lengths, temperature, feed rate, and particle velocity all play a significant effect. Exceptional process parameters for hardness is shown in Fig. 4.

2 Electrochemical Oxidation (EO)

Electrochemical reactions involve oxidation and reduction at the anode and cathode, primarily used for heavy metal remediation. These procedures remove pollutants through redox reactions at both the anode and cathode [29, 30]. Electro-oxidation is a wastewater treatment technique primarily used for industrial effluents. It involves two electrodes connected to a power source, forming strong oxidising types that degrade contaminants. Popular for its ease of setup and effectiveness, combining it with other technologies reduces operational costs whilst achieving high degradation standards.

Because anodic oxidation processes may result in partial or complete mineralization, the electrocatalytic properties

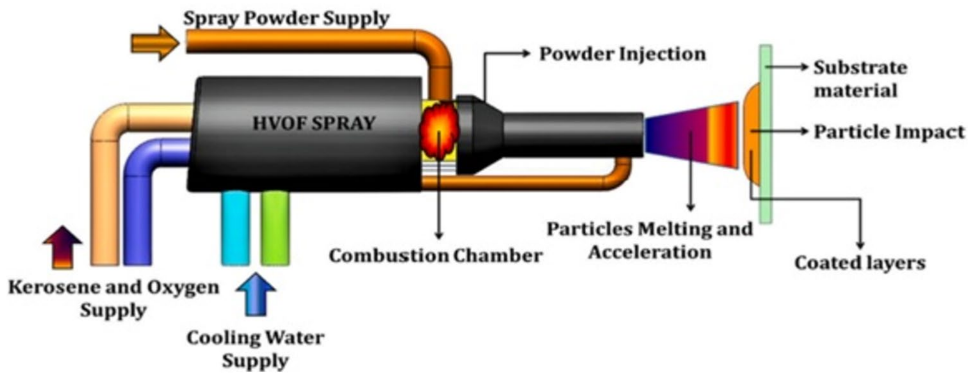

Fig. 3 HVOF spray process schematic view [18]

Table 2 Various process parameters of HVOF for different coating materials [103–116]

Coating material	Gas flow rate (LPM)	Feed rate of powder (gm/min)	Avg. particle temperature in °C	Avg. particle velocity (m/s)	Standoff distance (mm)	Hardness HV
NiCrSiBFe	240	45	2210	534	150	
NiCrAlY	250	42	900		240	563 ± 15
as-received NiCrAlY	210	38	1000	430	280	550 ± 15
nano-CeO_2 modified NiCrAlY	200	35	1000	430	250	450 ± 15
WC-10Co-4Cr	250–270	40	385		180	273.6
ASTM B338 Grade-5	250	30–50			200–250	
NiCoCrAlY	55–60	3	1100		180–220	
ZrB2–$MoSi_2$–SiC	200		1100		300	
WC-CoCr	280	65	1852	663	260	1355 ± 89
WC-Cr_3C_2-Ni	240	45		534	150	211 ± 2.3
WC-12Co	500	25–65	400		200–350	1260
WC-$10Co_4Cr$	500	25–65	600		200–350	1255
Cr_3C_2-25NiCr	500	25–65	750		200–350	1060
$Fe_{49.7}Cr_{18}Mn_{1.9}$ $Mo_{7.4}W_{1.6}B15.2C_{3.8}Si_{2.4}$	260	35	650		350	751.9

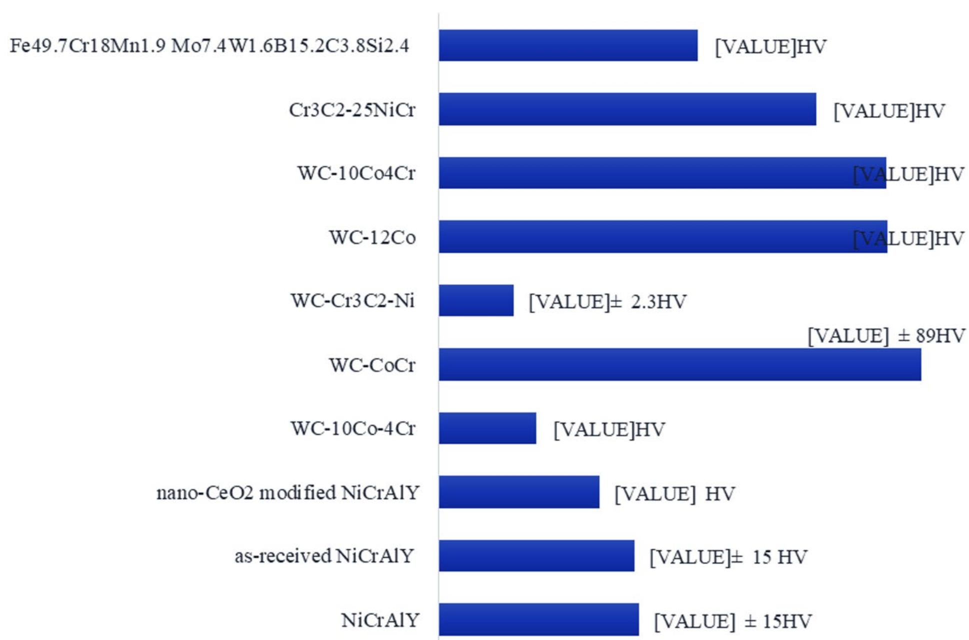

Fig. 4 Exceptional process parameters for hardness

of the anodic materials utilised have an impact on how well electrochemical procedures remove carbon-based pollutants [31–34]. The two different processes are indirect oxidation (ii) and direct anodic oxidation (i).

In order to stop combustion, carbon-based pollutants go through charge transfer processes in direct anodic oxidation or electrolysis. Applying potentials lower than the potential of the water oxidation process results in inhibition and surface poisoning. Similar to this, in situ electro-generation of a highly oxidant type mediates the indirect EO activities at the electrode surface [35]. Mixed metal oxides (MMOs) have been the subject of much heterogeneous catalysis research. Recent years have seen a significant increase in interest in MMOs as anode materials for the electrochemical treatment of waste waters, including refractory organic components [36]. There are two categories of MMOs: supported metal oxide anodes and bulk mixed metal oxide anodes. Different metal oxides may be deposited concurrently in bulk mixed metal oxide anodes using techniques, such as electro-deposition, chemical vapour deposition, physical vapour deposition, and thermochemical degradation. However, by combining metal oxides in the surface layer, supported MMO anodes seek to increase electrocatalytic performance and prolong service life [37, 38]. The surface composition of a binary metal oxide anode system is conceptually schematically shown in Fig. 5a. When all of the mixed MMO components are present in a bulk mixed metal oxide system, the MMO layer provides active sites for electrocatalytic processes. In the supported metal oxide anode, the layered structure of the supported oxide layer, dispersion layer, and active oxide layer is shown in Fig. 5b [39, 40].

2.1 Examining the Effects of Oxidation on HVOF Process Coatings

Hot oxidation is a process where salt contaminants, like NaCl, Na_2SO_4, and V_2O_5, combine to form molten deposits, destroying the protective surface oxide [41]. A number of variables, including contaminant, temperature, velocity, flux rate, erosion process, temperature cycle, and thermo-mechanical conditions, might affect the classification of it into hot- and low-temperature varieties [42]. High-temperature oxidation occurs between 850 and 950 °C, where fused alkali metal salt condenses to high temperature, causing chemical reaction that lowers the substrate materials chromium content. This results in rapid oxidation, proliferous scale, and the breaking of metallic components. Low-temperature oxidation occurs in the temperate region between 650 and 800 °C, causing pitting and sulphidation [43–46]. When the shielding oxide layer fails and liquid salt comes into contact with the substrate material, high-temperature oxidation takes place. Salt fluxing and sulphidation oxidation are two methods for producing hot oxidation [47, 48]. Researchers examined oxidation conditions and mechanical properties for coatings, discussing coating materials and substrates for HVOF process.

The illustration explains the oxidation mechanism of metal oxide nanostructures, where electrons are withdrawn from an anode, resulting in the formation of metal hydroxide and metal oxide. Thermal oxidation is a simple and high-yielding technique for growing metal oxide nanostructures, producing highly crystalline materials, easy patterning, scalability, and operating at atmospheric pressure. However, the main drawback is the long growth process time [49]. In Fig. 6a, the model for producing oxide scales in gaseous settings involves atomic oxygen adsorption on the metal surface, followed by the formation

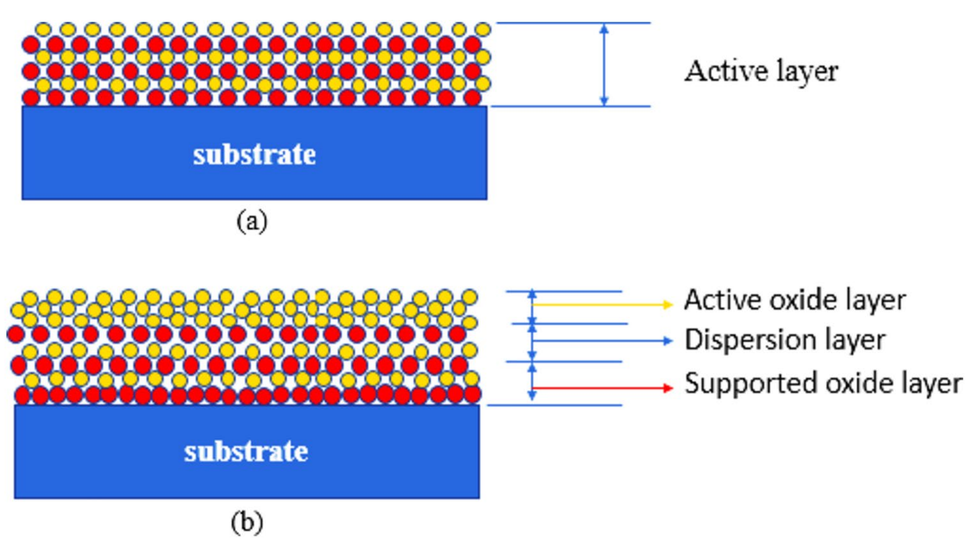

Fig. 5 Speculative diagram and surface oxides structures of **a** binary bulk mixed metal oxide anode and **b** supported metal oxide anode

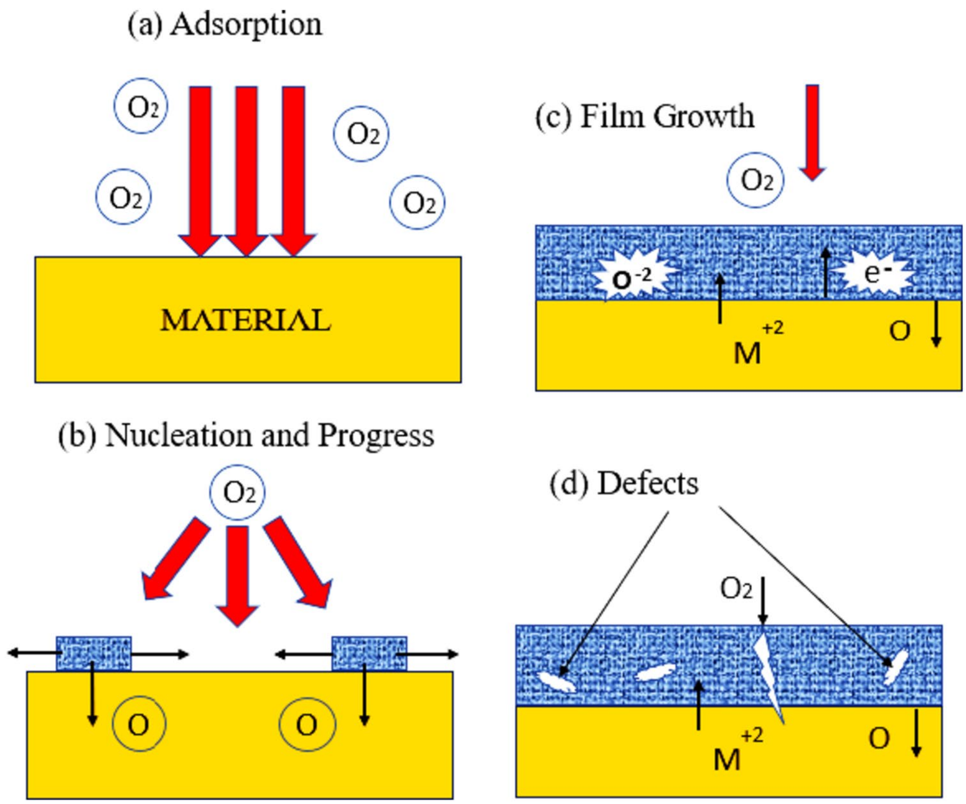

Fig. 6 Mechanism of oxidation. **a** Absorption, **b** Nucleation and progress, **c** Film growth, and **d** Defects

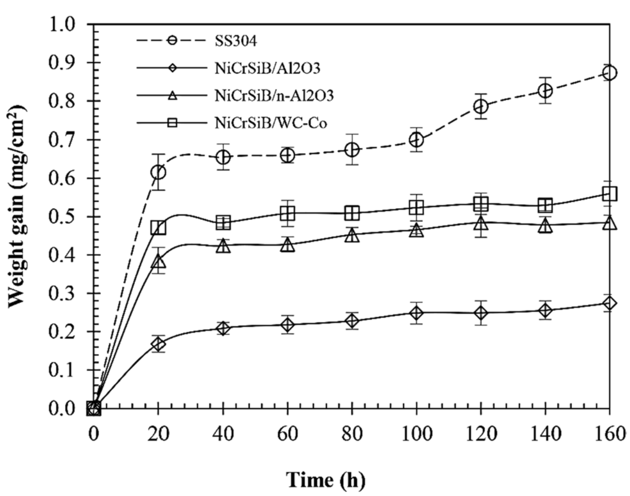

Fig. 7 Experimental evaluation of high-temperature oxidation reactions for HVOF coatings

of a thin oxide coating in Fig. 6b. Metal oxidation occurs as shown in Fig. 6c, releasing electrons that move through the oxide coating and react with atomic oxygen. Defects like porosity, voids, and micro cracks are caused by growing stresses and thickening of the oxide scale as shown in Fig. 6d.

In arrears to the detached and unprotected oxide scales on the steel surface, the mass gain of the SS304 sample was four times more than that of the NiCrSiB/Al_2O_3 sample sprayed with HVOF as shown in Fig. 7. The behaviour of oxidation deteriorated with time, reaching its maximum mass increase after 20 h. The coatings oxidative mass gain significantly increased after 20 h, showing the production of oxide at the surface, splat boundaries, and open pores. Oxides produced regularly on the surface, which resulted in constant rate of oxidation. On the other hand, the gradual increase in weight in the next cycles points to mass loss via carbon oxidation [50].

As part of valuation when oxidation occurs, the behaviour of microhardness was ascertained. Ni_3Ti and $Ni_3Ti + (Cr_3C_2 + 20NiCr)$ coatings on AISI 420 stainless steel and Ti-15 titanium alloy are produced using the HVOF technique. Figures 8 and 9 clarify the hardness line for substrates and coatings. When compared to $Ni_3Ti + (Cr_3C_2 + 20NiCr)$ coating, Ni_3Ti coating demonstrated greater microhardness on Ti-15 substrate. The strong cohesive strength, low porosity, and high density amongst individual splats are responsible for the enhanced microhardness value [51].

After 500 h of isothermal oxidation at 1273 K, the NiCoCrAlY-1W% nano-CeO_2 coatings show the formation of oxide scale, as explained by the scanning electron microscopy (SEM) picture. The layer of thermally graded oxides (TGO) has a compact structure and fully occupies the coated surface. TGO has an average thickness of around 2.0 μm,

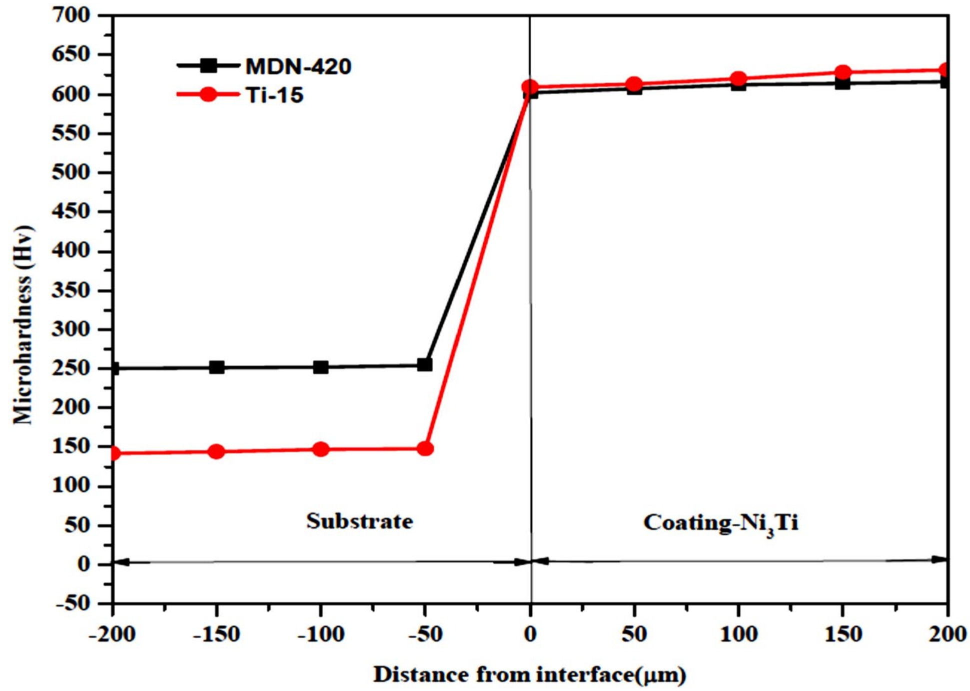

Fig. 8 Microhardness line for Ti-15 and MDN 420 substrates coated with Ni_3Ti, sprayed using HVOF

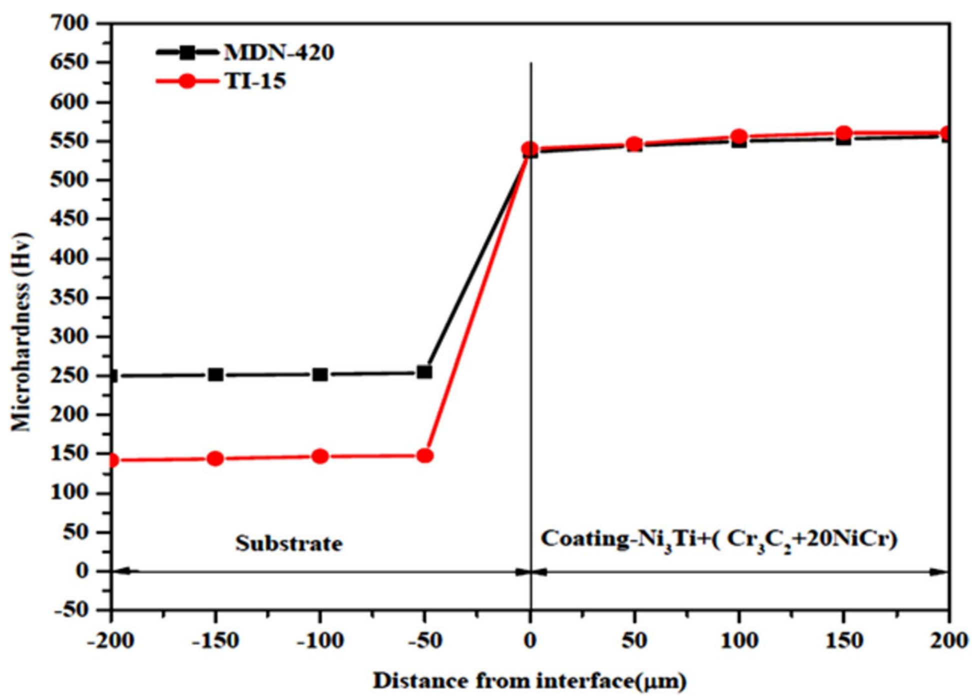

Fig. 9 Microhardness line $Ni_3Ti + (Cr_3C_2 + 20NiCr)$ coating sprayed by HVOF for MDN 420 and Ti-15 substrate

according to research on TGO growth. Phases may have a greater contrast if there are nano-CeO_2 clusters dispersed throughout the coating and inside the TGO layer. Because Ce has a limited solid solubility in MCrAlY, oxidation at 1273 K does not affect the chemical stability of nanoscaled CeO_2 oxide phases. [52] (Fig. 10).

A grey cast iron (GCI) substrate was successfully coated with a bi-layer of alloy-718/NiCrAlY utilising a high-velocity oxy-fuel technique. The microstructure of the coating was found to be more dense and low porosity than that of the untreated substrate, and it also had a higher microhardness value. The coating also showed reduced oxidation rate and little weight gain compared

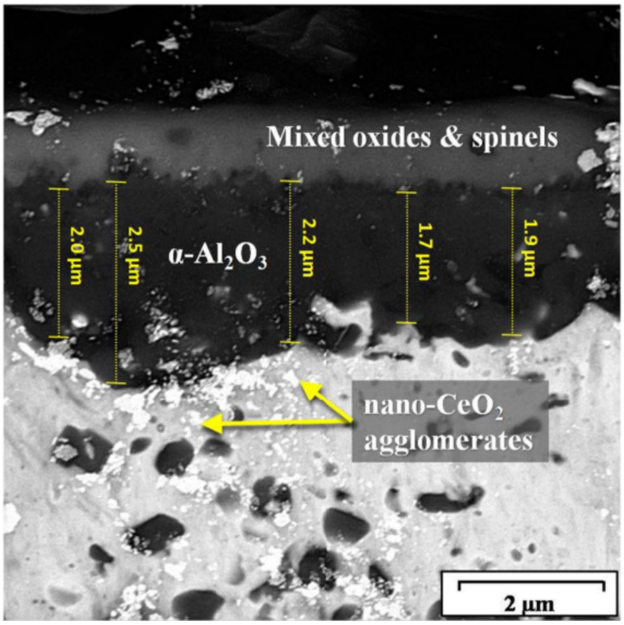

Fig. 10 FESEM cross-sectional micrograph of NiCoCrAlY-1W% nano-CeO_2 nanocomposite coatings

to the uncoated substrate. The development of protective phases like $NiCr_2O_4$, Al_2O_3, and Cr_2O_3 may contribute to the enhanced high-temperature oxidation resistance of the Alloy-718 coating. [53].

The microstructural properties of completely densified WC-Co particles in HVOF thermal covering on steel substrates. The feedstock powder, which lacks W_2C, contains Co_6W_6C and a minor amount of W_2C. The coating inhibits decarburization due to its densified microstructure. Low oxygen concentration of thick particles also prevents oxidation-induced decarburization. The porous feedstock powder's carbon interacts with oxygen to produce CO/CO_2 products. The completely densified feedstock powder allows most W and C atoms to precipitate as WC [54]. Thermally sprayed Cr_3C_2-NiCr coatings used to protect components from increased temperature wear because of coating resistance towards wear and high-temperature oxidation. These coatings are frequently used in boiler applications even though high temperatures marginally impair their strength and hardness. This study used an HVOF technique to mix a feedstock containing 70% FeNiCrMo and 30% SiC using ball milling in order to deposit the feedstock on ASTM-SA213-T-11. Because strong carbide phases formed to give microhardness and strength at high temperatures, the coating exhibited the lowest wear rate when compared to the substrate [55].

The weight increases for coated and uncoated items made of various coating materials with distinct substrates has been listed. Table 3 illustrates the assessment of HVOF approaches oxidation performance for different coated and uncoated substrates at 800 °C. In contrast, the oxidation performance of the HVOF approaches is valued for a range of coated and uncoated substrates at temperatures between 550 and 800 °C, as shown in Table 4 [56, 57].

Table 3 Covering Evaluation of HVOF techniques oxidation performance for various layered and base materials at 800 °C [117–124]

Coating materials	Base material	Uncoated (mg/cm^2)	Coated (mg/cm^2)
Ni-20Cr	T-22	136	53.04
Cr_3C_2-NiCr	SN 600	15	8.25
Ni-20Cr	SN 600	15	6
NiCr	GrA1	349.4	10.6
NiCr	T-11	234.4	13.8
NiCr	T-22	426.1	20
NiCrBSi	SN 718	7	9.45
NiCrBSi	SN 75	8	6.32
NiCrBSi	SN 601	26	9.4
Cr3C2-NiCr	SN 601	26	8.3
Ni-20Cr	SN 601	26	6.5
Stellite-6	SN 601	26	10.4
Ni-20Cr	T-22	49.7	12.2
Ni-20Cr	T-91	2.07	1.5
Cr3C2-25(Ni-20Cr)	T-91	2.07	0.4
Ni-20Cr	347H	3	0.8
Satellite-6	SN 600	16	12.6

Table 4 Evaluation of various layered and base materials oxidation performance at temperature 550–800 °C [117–124]

Coating materials	Base material	Uncoated (mg/cm^2)	Coated (mg/cm^2)
NiCrC nano	ASTM1020 Steel	13	0.1
NiCrC Conventional	ASTM1020 Steel	13	0.28
NiCrC nano	ASTM1020 Steel	34	1
NiCrC Conventional	ASTM1020 Steel	34	1.5
Cr_3C_2-NiCr	31OS	6	3.99
Cr_3C_2-NiCr	T-22	77.87	3.83
Cr_3C_2-NiCr	SAE-347H	6.174	2.95
Cr_3C_2-35%NiCr + 5% Si	T-22	24.71	7.05
Cr_3C_2-35%NiCr + 5% Si	MDN-310	3.97	4.43
Cr_3C_2-35%NiCr + 5% Si	SF 800H	3.15	3.5
NiCrC nano [109]	ASTM1020 Steel	108	1.1
NiCrC Conventional [109]	ASTM1020 Steel	108	1.31
Al_2O_3-40% TiO_2 [113]	SN 601	56.81	51.36
Al_2O_3-40% TiO_2 [113]	SN 605	52.02	49.39
Al_2O_3 + CoCrAlTaY [114]	Ti-31	72.3	10.3
WC-NiCrFeSi [115]	SN 75	110	40

3 Performance of Coatings Against Hot Corrosion and Erosion Using HVOF Technique

Hot corrosion is a complex, accelerated phenomenon affecting materials in industries, like aerospace, energy, and chemical processing [58]. It is caused by salt deposits, typically sodium sulphate, dissolving the protective oxide layer and exposing it to aggressive oxidation. Deterioration is natural process of material weakening and loss due to oxides, sulphides, and hydroxides [58–60]. Whereas, erosion is surface deprivation caused by mechanical actions. Erosive wear is significant degradation mechanism in engineering systems, like gas turbine engines, thermal power plants, and coal slurry pipe lines [61]. To improve resistance, coatings can be used on superalloy components to address erosion problems and strengthen them at elevated temperatures [62].

Samples were subjected to hot corrosion testing after the deposition of NaCl at 750 °C, which produced ideal conditions for hot corrosion at rapidly varying temperatures [63–65]. A minimum of 3 specimens were analysed in order to guarantee the reproducibility of the results. The corrosion dynamics of the alloys were examined using mass gain measurements. Figure 11 depicts the alloys' weight change kinetics after 15 cycles. The A1, A2, and A3 alloys clearly lost weight when exposed to NaCl corrosion, whilst the A4 alloy did not lose weight even after 150 h [66]. The A4 alloy showed a weight increase of 0.56 mg cm $-^{2}$ and its kinetic curve began to decline after three cycles. A1 alloy had a weight change that was similar to A2, whereas A3 alloy had a weight change of − 10 mgcm $-^{2}$. In the heated corrosion test, the A3 alloy demonstrated greater stability, indicating that the mass loss for alloys reduced as the Mo concentration increased [67].

The study assesses the lifetime and failure mechanisms of metal link coats thermal barrier coatings (TBC) systems based on titanium and CoNiCrAlY, which are generated on nickel-based Inconel 718 superalloy substrates using

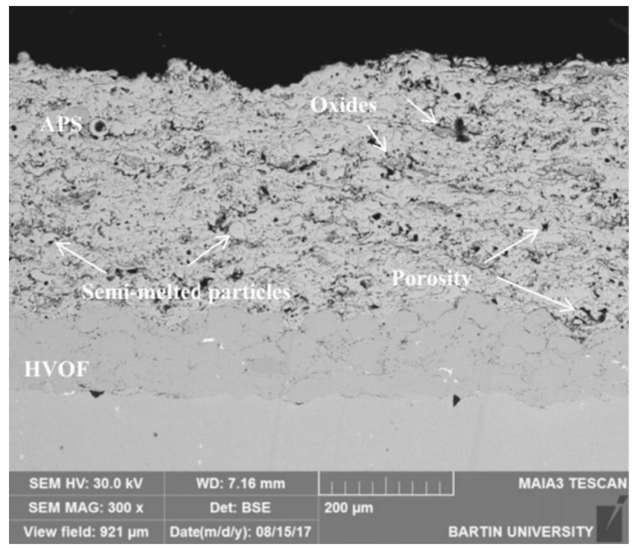

Fig. 12 The cross-sectional micrograph for YSZ TBC created using APS method shows an as-sprayed coat of HVOF CoNiCrAlY

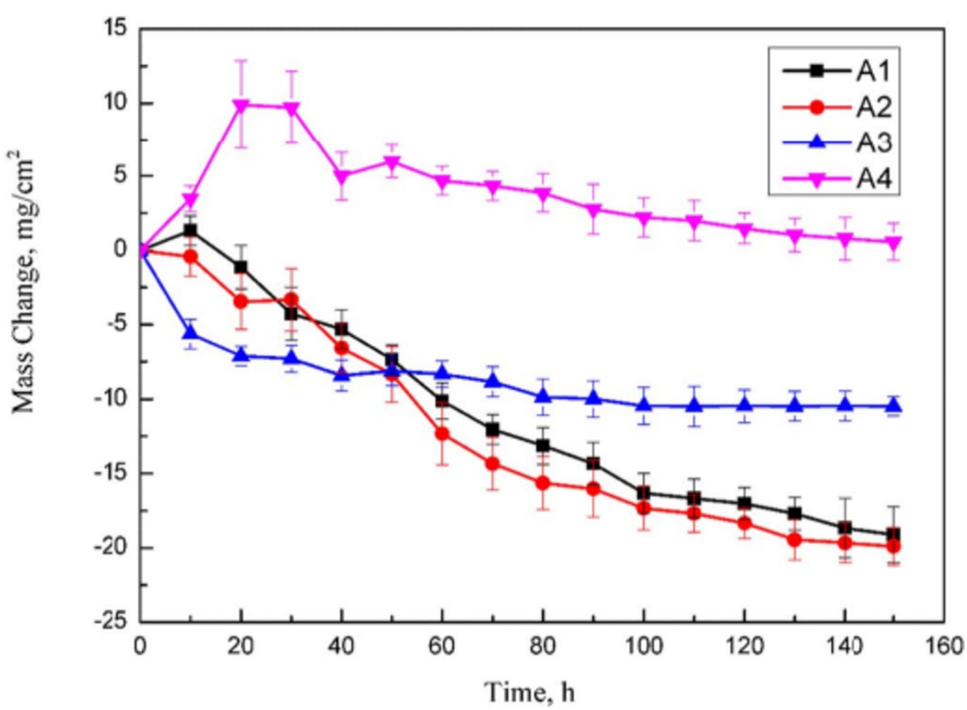

Fig. 11 Kinetic curves of A1–A4 hot corrosion caused by NaCl at 750 °C

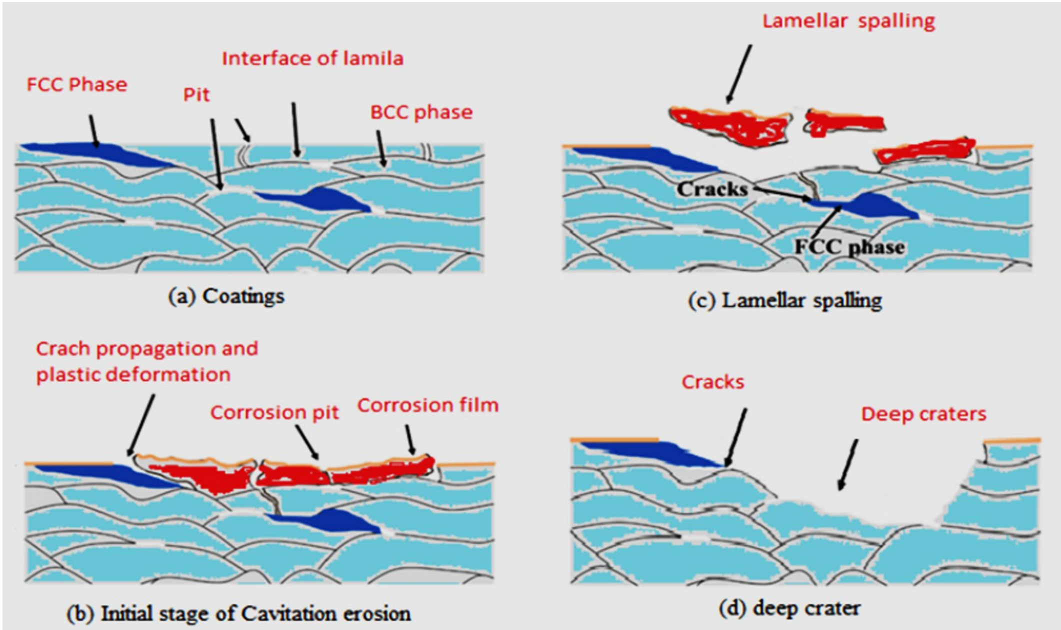

Fig. 13 Schematic diagram of cavitation erosion mechanism of the HEA coating in 3.5-wt% NaCl solution

Atmospheric plasma spray (APS) and HVOF procedures. An APS method cross-sectional micrograph of YSZ TBCs with HVOF CoNiCrAlY tie coat is shown in Fig. 12. The APS approach produced microstructures for TBC that are porous, cracked, and had discontinuous apertures. On the other hand, microstructures of TBC produced by the HVOF process are evaluated when TBC is sprayed. They are less oxide- and porosity containing [68].

The cavitation erosion mechanism of the HEA coating in a 3.5-wt% NaCl solution is illustrated in Fig. 13, with deep craters appearing on pits and interfaces. The main mechanism is lamellar spalling, increasing cracks and accelerating local spalling. Under micro-jet impact, the coating's surface deforms, causing stress concentration and crack growth. Corrosion damage is aggravated by the interface between the FCC phase and BCC phase. Pitting corrosion is more common on the eroded surface of 06Cr13Ni5Mo steel. [69].

In molten salt environment of Na_2SO_4–60% V_2O_5, at 900 °C, a hot corrosion investigation was conducted on the uncoated and Ni–20% Cr-coated superalloy 825. Optical microscope and SEM/EDS on behalf of elemental enquiry were used to study the cross-sectional morphology of hot-corroded, hot-coated, and uncoated superalloy following 50 cycles of exposure to molten salt at 900 °C. At 63.09 µm and

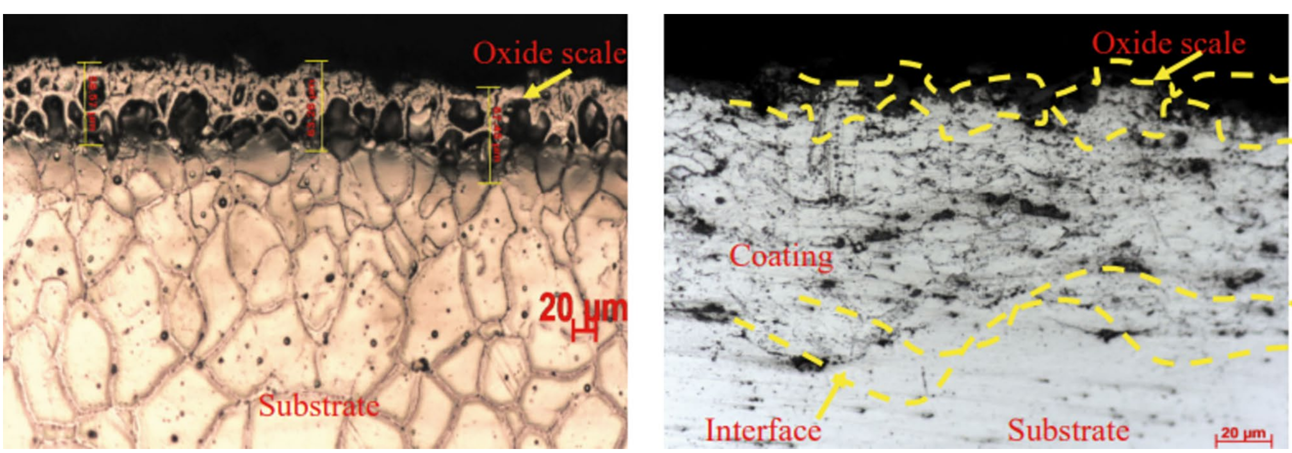

Fig. 14 Optical microscope cross-section picture of Ni-based superalloy after 50 cycles of exposure to a Na_2SO_4-60%V_2O_5 atmosphere at 900 °C. **a** Bare 825 and **b** Ni-20Cr-coated Superalloy [70]

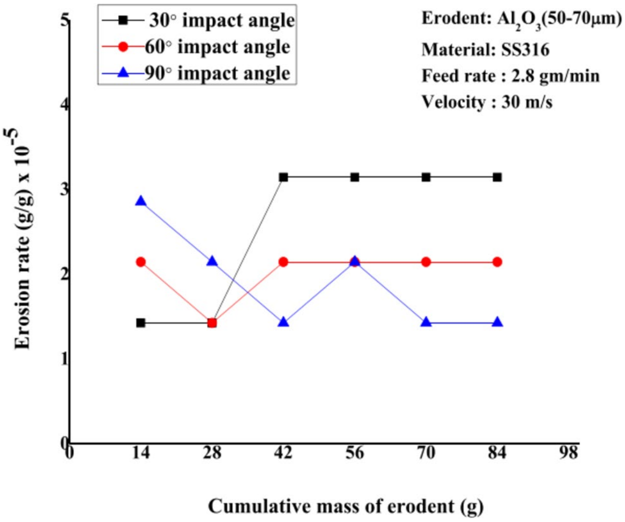

Fig. 15 Variation in uncoated SS316 steel's rate of incremental erosion at impact angles of 30°, 60°, and 90°

8.64 µm in thickness, respectively, the oxide scales on the untreated and HVOF-coated specimens were thicker. There were also visible cracks and the depth of attack as depicted in Fig. 14a and b. Vital information on the characteristics of hot-corroded superalloy is provided by the study [70].

Using HVOF and low vacuum plasma spray (LVPS) method, a hot corrosion performance test was performed on an Inconel-738 substrate coated with CoNiCrAlYSi. Using molten film containing 20-weight percent NaV_2O_3, samples of various coating processes were evaluated for roughly 560 h at high temperature 880 °C. The study evaluated hot corrosion performance using mass gaining analysis. LVPS coatings experienced weight change in three stages, but HVOF spray method shielded hot corrosion for the entire duration, proving superior to LVPS [71].

For the duration for coating process, the HVOF deposition spraying parameters were kept constant. Based on the ASTM G76-02 specification, Figures 15 and 16 depict the balanced state, volume erosion, and its rate as a function of rate of impact angle and cumulative mass for erodent, respectively. The graph shows that 90° is the highest impact angle and 30° is the lowest angle, and the rate of degradation is stabilised. Elevated surface roughness played a major role in initial transient. The balanced volume erosion rate for coatings remained larger at 90° than 30° and erosive loss for brittle materials stayed greater at 90° than 30° [72–75].

The HVOF spraying process effectively deposited Inconel 625 and Inconel 718 coatings for T-22 boiler steel. However, significant weight growth and oxide layer spalling were observed, possibly due to high iron content in the steel. Fe_2O_3 and chlorine gas were produced when environmental chlorine created volatile metal chlorides. The main phases identified from HVOF-sprayed Inconel 625 and Inconel 718

Fig. 16 Variation in incremental erosion rate at 30°, 60°, and 90° for coatings with WC-Co/Ni Cr Al Y Si (35–65%)

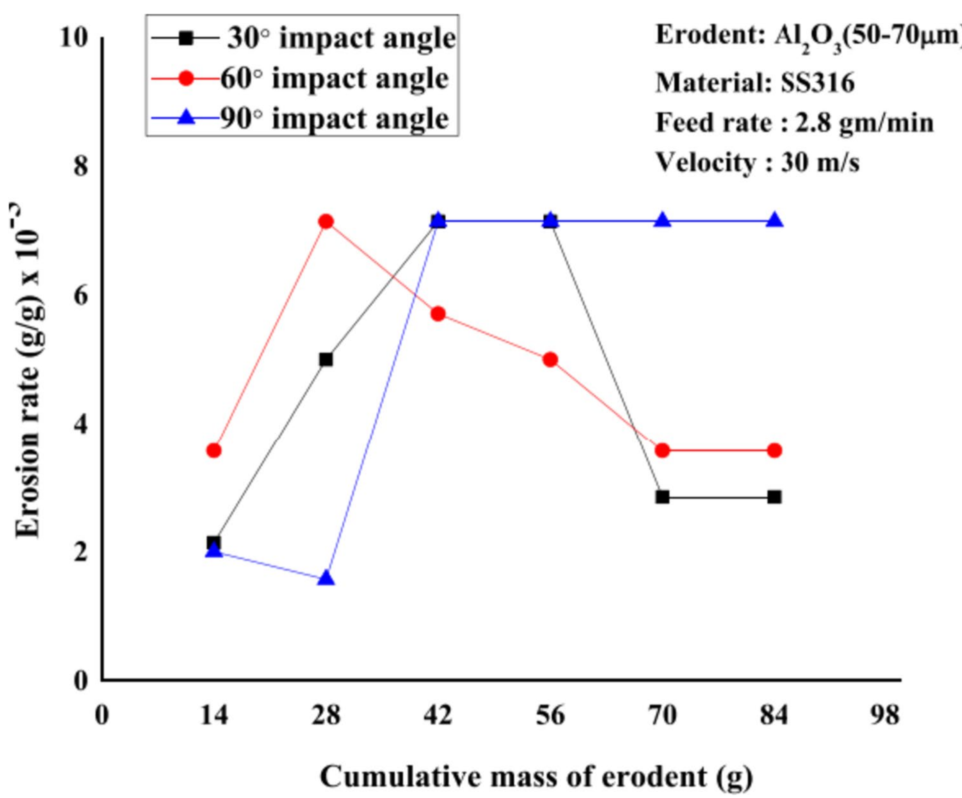

Table 5 The study evaluates the corrosion and erosion of various coating compositions under various operating conditions [125–132]

Base material	Coating powder	Post-process	Testing particles	Grain size	Investigational duration	Experimental	Material loss
UNS-G41350 steel	Cr_3C_2–NiCr and WC–Ni	As sprayed and Polished	Mixture of 0.25-wt% sand and 3.4-wt% NaCl	250 µm	24r	22.9 m/s 20 °C 14.3 m/s 20 °C	2.8/1.4 cm^3/year 0.7/0.6 cm^3/year
HP steel	NiAl and CeO_2	Heat treated at 600 °C	AFS 50/70 Test Sand		60 h	Room temperature, Abrasive flow, 80 g/min at 900 °C	(erosion rate/ %Ceo_2) g/g × 106 2/2, 2.2/4.7, 3.7/8
Superni 76 Superni 750 Superfer 800	NiCrAl		Na_2SO_4–60% V_2O_5		1 h	900 °C/100 cycle	(mass gain gm/ cm^2) base metal/coated 35/12, 34/4, 30/10
Steel	Cr_3C_2-50(Ni-20Cr)	Annealed at 400 °C, 600 °C, 800 °C	silica erodent particles	150 µm to 300 µm	5 min break till steady state condition	Velocity 45 m/s at 900^0C	($\times 10^{-3}$ gm/gm) 0.15, 0.085, 0.06, 0.078
IN738LC superalloy	CoNiCrAlYSi		Na_2SO_4- 20-Wt% Na V_2O_3	0.5 to1 g/cm^2	560 h	880^0C with intervals of 20 h	Mass change (mg/ cm^2) 3.5/100 h 5.4/300 h 5.3/500 h
AISI 316 Molybdenum steel	Cr_3C_2–NiCr (85/15, 90/10, & 95/05%)		Abrasive flux silica		10 min at 75° impact angle	Velocity 80 m/s at 650 °C	(mg/g × 10^{-7}) 2.8, 3.2, 4.4
Low carbon steel ASTM-SA210	35%WC–Co/NiCr-FeSiB		Silica sand	125 to180µm	Cycles of 5 min	Room temperature at 300/900 impact angle	Erosion/cumulative mass (g/g × 10^{-5}) 0.5/25, 9/25, 16/25, 19/25
23–8-N Nitronic steel	WC-10Co-4Cr	Solution treated (1220 °C/150 min)	Flaky- and angular-type alumina particles	50 µm	10 min	30^0 and 90° impact angles at room temperature	Vol. loss/mass of particle cm^3/g $1\times e^{-4/5}$, $1.5\times e^{-4/15}$, $2.5\times e^{-4/25}$
AISI 430 and AISI 204	Cr_3C_2-25NiCr		Sand water mixture	550 µm	60 min	30° and 90° impact angle at 40 to 45 °C	Weight loss mg/hr 3/3/1 h, 6/6/3 h, 14/13.5/6 h
Alloy steel	SAF2507 Super duplex alloy, boron, Fe–B		35 g/L NaCl		30 min	Room temperature	Vol. loss mm^3 22, 8, 6, 4
Steel alloy	CeO_2 modified WC-12Co powder		Silica sand 3.5-wt% NaCl & 1 mol/LH_2SO_4	500 µm	8 h	Room temperature	Corrosion rate gm^{-2} h^{-1} 0.0205, 0.0316, 0.0498
Alloy steel	WC-40Cr_3C_2-25NiCr, WC-10Co_4Cr, Cr_3C_2-25NiCr	Electrolytic hard chrome	SiO_2		45 min	Room temperature (150 g/min)	Volume loss at 300 mm^3/min 0.18, 0.27, 0.45, 0.34

were Cr_2O_3, $NiCr_2O_4$, K_2CrO_4, Ni, and NiS, with Na_2CrO_4 peaks in Inconel 625 and Fe_2O_3 in Inconel 718 [76–82].

AISI 316 austenitic steel plates were coated using the HVOF spray technique with a Cr_3C_2/NiCr composition in three different weight ratios, i.e. A (85/15) %, B (90/10) %, and C (95/10) %. The erosion wear test was conducted in an atmosphere with a high temperature of approximately 650 °C and three different impact angles: 60°, 75°, and 90°. Because sample angles composition has a smaller amount of carbide, it exhibits excellent erosion resistance qualities. Additionally, sample erosion wear rate is also lower at 75° angles of impingement for every sample [83–89].

A material will naturally weaken and lose some of its properties due to oxide, sulphide, and hydroxide. This process is called corrosion. Erosion is the mechanical deterioration of a surface caused usually by liquid impinging, abrasion through a slurry, elements deferred from gas or fluid that flows quickly, foams, droplets, etc. [90–92]. Table 5 presents the corrosion and erosion performance conducted by multiple researchers.

An analysis of the erosion and erosion-corrosion characteristics of MoNbTaTiZr and SS316L high-entropy alloys (HEA) under oblique lighting circumstances. In erosive circumstances, the HEA exhibited greater resilience and lower rates of erosion than stainless steel. Under typical impact situations, however, erosion rates somewhat increased. Additionally, the HEA showed far greater resistance to erosion and corrosion—more than 3.5 times better than that of stainless steel. Its increased hardness, which restricts material removal by reducing the mobility of abrasive particles during shearing action and offers protection against slurry erosion and corrosion, is principally responsible for its superior erosion and corrosion resistance [93–96].

4 Conclusion

This literature included insights on how the HVOF spray method was used to change the surface of several components from a number of applications, including the paper, aerospace, chemical, gas turbine, automobile, and nuclear power plant sectors, via its characteristics and spray parameters. This technology is adaptable and may lower coating costs, according to ongoing research and development.

The authors have derived their conclusions from the literature.

- HVOF spraying method enhances component surface qualities in aggressive environments, is cost-effective, compact, and has low porosity, achieving 200-micron coating thickness without oxide formation.
- The study compared the oxidation, corrosion, and erosion performance of HVOF at high temperatures. The HVOF-sprayed coating showed greater protection, whilst adhesion properties varied depending on coating method and post-treatment. The heat-treated HVOF coating method achieved superior adhesion properties, as per previous research.
- HVOF spray technique improves metal component surface properties with mixture of nano- and micro-sized particle, overcoming the cost and carbon-repellent issues of nano-sized particles alone.
- Investigations on mixed compositions using HVOF spray technique are ongoing. Impending studies have to consider altered weight percentages and post-treatment compositions.
- Important parameters that affect the qualities of coatings and have an influence on the HVOF spray process. Different spray settings compress the features of the coating.

Author contributions S.K.S wrote the manuscript and prepared figures, C.D.P complied all the data and then analysed and reviewed the manuscript, and H.H prepared figures and reviewed manuscript.

Funding Authors would like to thank Science and Engineering Research Board (SERB) for financial support to carry out this research work. Project File no: CRG/2022/004140, under Core Research Grant (CRG) scheme, Government of India.

Data Availability No datasets were generated or analysed during the current study.

Declarations

Competing Interests The authors declare that they have no conflicts of interest.

References

1. Praveen AS, Arjunan A (2022) High-temperature oxidation and erosion of HVOF sprayed NiCrSiB/Al_2O_3 and NiCrSiB/WCCo coatings. Appl Surf Sci Adv 7:100191
2. Doleker KM, Ozgurluk Y, Kahraman Y, Karaoglanli AC (2021) Oxidation and hot corrosion resistance of HVOF/EB-PVD thermal barrier coating system. Surf Coat Technol 409:126862
3. Sadeghi E, Joshi S (2019) Chlorine-induced high-temperature corrosion and erosion-corrosion of HVAF and HVOF-sprayed amorphous Fe-based coatings. Surf Coat Technol 371:20–35
4. Picas JA, Punset M, Rupérez E, Menargues S, Martin E, Baile MT (2019) Corrosion mechanism of HVOF thermal sprayed WC-CoCr coatings in acidic chloride media. Surf Coat Technol 371:378–388
5. Abu-Warda N, López AJ, López MD, Utrilla MV (2020) Ni20Cr coating on T24 steel pipes by HVOF thermal spray for high temperature protection. Surf Coat Technol 381:125133
6. Pradeep DG, Venkatesh CV, Nithin HS (2022) Review on tribological and mechanical behavior in HVOF thermal-sprayed

composite coatings. J Bio Tribo Corros 8:30. https://doi.org/10.1007/s40735-022-00631-x

7. Avci A, Eker AA, Eker B (2018) Microstructure and oxidation behavior of atmospheric plasma-sprayed thermal barrier coatings. Exergetic, energetic and environmental dimensions. Academic Press, Elsevier, pp 793–814
8. Sahith MS, Giridhara G, Suresh Kumar R (2018) Development and analysis of thermal barrier coatings on gas turbine blades–a review. Mater Today: Proceed 5(1):2746–2751
9. Demirci M, Bagci M (2022) Erosion of ceramic coating applications under the influence of APS and HVOF methods. Appl Nanosci 12(11):3409–3415
10. Suresh Babu P, Madhavi Y, Rama Krishna L, Sivakumar G, Srinivasa Rao D, Padmanabham G (2020) Thermal spray coatings for erosion–corrosion resistant applications. Trans Ind Inst Metals 73:2141–2159
11. Bolelli G, Bursi M, Lusvarghi L, Manfredini T, Matikainen V, Rigon R, Sassatelli P, Vuoristo P (2018) Tribology of FeVCrC coatings deposited by HVOF and HVAF thermal spray processes. Wear 394:113–133
12. Hajare AS, Gogte CL (2018) Comparative study of wear behaviour of Thermal Spray HVOF coating on 304 SS. Mater Today: Proceed 5(2):6924–6933
13. Singh S, Kumar R, Goel P, Singh H (2022) Analysis of wear and hardness during surface hardfacing of alloy steel by thermal spraying, electric arc and TIG welding. Mater Today: Proceed 50:1599–1605
14. Kumar S, Kumar R (2021) Influence of processing conditions on the properties of thermal sprayed coating: a review. Surf Eng 37(11):1339–1372
15. Song Bo, Murray JW, Wellman RG, Pala Z, Hussain T (2020) Dry sliding wear behaviour of HVOF thermal sprayed WC-Co-Cr and WC-CrxCy-Ni coatings. Wear 442:203114
16. Ham GS, Kreethi R, Kim HJ, Yoon SH, Lee KA (2021) Effects of different HVOF thermal sprayed cermet coatings on tensile and fatigue properties of AISI 1045 steel. J Mater Res Technol 15:6647–6658
17. Tillmann W, Kuhnt S, Baumann IT, Kalka A, Becker-Emden EC, Brinkhoff A (2022) Statistical comparison of processing different powder feedstock in an HVOF thermal spray process. J Therm Spray Technol 31(5):1476–1489
18. Seraj RA, Abdollah-zadeh A, Dosta S, Assadi H, Cano IG (2019) Comparison of stellite coatings on low carbon steel produced by CGS and HVOF spraying. Surf Coat Technol 372:299–311
19. Mittal G, Paul S (2022) Suspension and solution precursor plasma and HVOF spray: A review. J Therm Spray Technol 31(5):1443–1475
20. Murariu AC, Pleşu N, Perianu IA (2017) Investigations on corrosion behaviour of WC–CrC–Ni coatings deposited by HVOF thermal spraying process. Int J Electrochem Sci 12(2):1535–1549
21. Gui M, Eybel R, Radhakrishnan S, Monerie-Moulin F, Raininger R, Taylor P (2019) Residual stress in HVOF thermally sprayed WC-10Co-4Cr coating in landing gear application. J Therm Spray Technol 28(6):1295–1307
22. Kiilakoski J, Trache R, Björklund S, Joshi S, Vuoristo P (2019) Process parameter impact on suspension-HVOF-sprayed Cr_2O_3 coatings. J Therm Spray Technol 28:1933–1944
23. Pukasiewicz AGM, De Boer HE, Sucharski GB, Vaz RF, Procopiak LAJ (2017) The influence of HVOF spraying parameters on the microstructure, residual stress and cavitation resistance of FeMnCrSi coatings. Surf Coat Technol 327:158–166
24. Rajendran PR, Duraisamy T, Seshadri RC, Mohankumar A, Ranganathan S, Balachandran G, Murugan K, Renjith L (2022) Optimisation of HVOF spray process parameters to achieve minimum porosity and maximum hardness in WC-10Ni-5Cr coatings. Coatings 12(3):339
25. Srinath MK, Nagendra J (2022) Post-processing parameter optimization to enhance the surface finish of HVOF-developed coatings. Multiscale Multidiscip Model, Exp Des 5(3):255–267
26. Rukhande SW, Rathod WS (2020) Tribological behaviour of plasma and HVOF-sprayed NiCrSiBFe coatings. Surf Eng 36(7):745–755
27. Schab JC, Zimmermann JRA, Grasso P-D, Stankowski A, Heinze S, Marquardt A, Leyens C (2019) Thermodynamic calculation and experimental analysis of critical phase transformations in HVOF-sprayed NiCrAlY-coating alloys. Surf Coat Technol 357:924–938
28. Ghadami F, . Sabour Rouh Aghdam A (2020) Preparation of NiCrAlY/nano-CeO2 powder with the core-shell structure using high-velocity oxy-fuel spraying process. Mater Chem Phys 243:122551
29. Garcia-Segura S, Ocon JD, Chong MNan (2018) Electrochemical oxidation remediation of real wastewater effluents—A review. Process Saf Environ Prot 113:48–67
30. Galedari SA, Mahdavi A, Azarmi F, Huang Y, McDonald A (2019) A comprehensive review of corrosion resistance of thermally-sprayed and thermally-diffused protective coatings on steel structures. J Therm Spray Technol 28:645–677
31. Santos D, Jhones A, Garcia-Segura S, Dosta S, Cano IG, Martínez-Huitle CA, Brillas E (2019) A ceramic electrode of ZrO2-Y2O3 for the generation of oxidant species in anodic oxidation. Assessment of the treatment of Acid Blue 29 dye in sulfate and chloride media. Sep Purif Technol 228:115747
32. Ajayi BP, Thapa AK, Cvelbar U, Jasinski JB, Sunkara MK (2017) Atmospheric plasma spray pyrolysis of lithiated nickel-manganese-cobalt oxides for cathodes in lithium ion batteries. Chem Eng Sci 174:302–310
33. Waluyo NS, Park SS, Song RH, Lee SB, Lim TH, Hong JE, Ryu KH, Im WB, Lee JW (2018) Protective coating based on manganese–copper oxide for solid oxide fuel cell interconnects: plasma spray coating and performance evaluation. Ceram Int 44(10):11576–11581
34. Shestakova M, Sillanpää M (2017) Electrode materials used for electrochemical oxidation of organic compounds in wastewater. Rev Environ Sci Bio/Technol 16:223–238
35. Zhu Y, Zuwei Xu, Yan K, Zhao H, Zhang J (2017) One-step synthesis of CuO–Cu2O heterojunction by flame spray pyrolysis for cathodic photo electrochemical sensing of l-cysteine. ACS Appl Mater Interfaces 9(46):40452–40460
36. Wu J, Zhang SD, Sun WH, Wang JQ (2018) Influence of oxidation related structural defects on localized corrosion in HVAF-sprayed Fe-based metallic coatings. Surf Coat Technol 335:205–218
37. Chen Y, Zhao X, Xiao P (2018) Effect of microstructure on early oxidation of MCrAlY coatings. Acta Mater 159:150–162
38. Han Y, Zhu Z, Zhang B, Chu Y, Zhang Y, Fan J (2018) Effects of process parameters of vacuum pre-oxidation on the microstructural evolution of CoCrAlY coating deposited by HVOF. J Alloys Compds 735:547–559
39. Kalush A, Texier D, Ecochard M, Sirvin Q, Choquet K, Gheno T, Vanderesse N, Jomaa W, Bocher P (2022) Size effects on high temperature oxidation of MCrAlY coatings processed via APS and HVOF depositions. Surf Coat Technol 440:128483
40. Karaoglanli AC, Ozgurluk Y, Doleker KM (2020) Comparison of microstructure and oxidation behavior of CoNiCrAlY coatings produced by APS, SSAPS, D-gun, HVOF and CGDS techniques. Vacuum 180:109609
41. Fan L, Zhu B, Pei-Chen Su, He C (2018) Nanomaterials and technologies for low temperature solid oxide fuel cells:

recent advances, challenges and opportunities. Nano Energy 45:148–176
42. Song B, Bai M, Voisey KT, Hussain T (2017) Role of oxides and porosity on high-temperature oxidation of liquid-fueled HVOF thermal-sprayed Ni50Cr coatings. J Therm Spray Technol 26:554–568
43. Hao E, Zhao X, An Y, Deng W, Zhou H, Chen J (2019) The effect of pre-oxidation on microstructure, mechanical properties and high-temperature tribological behaviors of HVOF-sprayed NiCoCrAlYTa coating. Appl Surf Sci 489:187–197
44. Feizabadi A, Salehi Doolabi M, Sadrnezhaad SK, Rezaei M (2018) Cyclic oxidation characteristics of HVOF thermal-sprayed NiCoCrAlY and CoNiCrAlY coatings at 1000° C. J Alloys Compds 746:509–519
45. Reddy NC, Ajay Kumar BS, Reddappa HN, Ramesh MR, Koppad PG, Kord S (2018) HVOF sprayed Ni3Ti and Ni3Ti+ (Cr_3C_2+ 20NiCr) coatings: Microstructure, microhardness and oxidation behaviour. J Alloys Compds 736:236–245
46. Dzhurinskiy D, Babu A, Pathak P, Elkin A, Dautov S, Shornikov P (2021) Microstructure and wear properties of atmospheric plasma-sprayed Cr_3C_2-NiCr composite coatings. Surf Coat Technol 428:127904
47. Reddy NC, Ajay Kumar BS, Ramesh MR, Koppad PG (2018) Microstructure and adhesion strength of Ni 3 Ti coating prepared by mechanical alloying and HVOF. Phys Metals Metallogr 119:462–468
48. Ghadami F, Zakeri A, Sabour Rouh Aghdam A, Tahmasebi R (2019) Structural characteristics and high-temperature oxidation behavior of HVOF sprayed nano-CeO_2 reinforced NiCoCrAlY nanocomposite coatings. Surf Coat Technol 373:7–16
49. Vasudev H, Thakur L, Bansal A, Singh H, Zafar S (2019) High temperature oxidation and erosion behaviour of HVOF sprayed bi-layer alloy-718/NiCrAlY coating. Surf Coat Technol 362:366–380
50. Tillmann W, Hagen L, Schaak C, Liß J, Schaper M, Hoyer K-P, Aydinöz ME, Garthe K-U (2020) Adhesion of HVOF-sprayed WC-Co coatings on 316L substrates processed by SLM. J Therm Spray Technol 29:1396–1409
51. Singh J, Vasudev H, Singh S (2020) Performance of different coating materials against high temperature oxidation in boiler tubes–a review. Mater Today: Proceed 26:972–978
52. Raza A, Ahmad F, Badri TM, Raza MR, Malik K (2022) An Influence of oxygen flow rate and spray distance on the porosity of HVOF coating and its effects on corrosion—a Review. Materials 15(18):6329
53. Sabanayagam S, Chockalingam S (2020) Analysis of high temperature oxidation behaviour of SS316 by Al2O3 and Cr_2O_3 coating. Mater Today: Proceed 33:2641–2645
54. Sharma V, Kumar S, Kumar M, Deepak D (2020) High temperature oxidation performance of Ni-Cr-Ti and Ni-5Al coatings. Mater Today: Proceed 26:3397–3406
55. Kumar S, Kumar M, Handa A (2018) Combating hot corrosion of boiler tubes–a study. Eng Fail Anal 94:379–395
56. Ansari MS, Bansal A, Chawla V, Aggarwal V (2021) Comparative study of hot corrosion behavior of bare and plasma sprayed Al2O3–40% TiO2 coated T-91, A-1 boiler steel and Superfer800H superalloy in Na2SO4–60% V2O5 salt environment. Surface Topogr: Metrol Prop 9(2):025029
57. Patil VG, Somasundaram B, Kandaiah S, Kumar S (2022) High temperature corrosion behavior of high velocity oxy fuel sprayed NiCrMoFeCoAl-30% SiO_2 and NiCrMoFeCoAl-30% Cr_2O_3 composite coatings on ASTM SA213-T22 steel in a coal-fired boiler environment. Int J Eng 35(7):1416–1427
58. Madhusudana Reddy G, Durga Prasad C, Patil P, Kakur N, Ramesh MR (2023) Investigation of plasma sprayed NiCrAlY/Cr_2O_3/YSZ coatings on erosion performance of MDN 420 steel substrate at elevated temperatures. Int J Surf Sci Eng 17(3):180–194. https://doi.org/10.1504/IJSURFSE.2023.10054266
59. Sharanabasva H, Durga Prasad C, Ramesh MR (2023) Effect of Mo and SiC reinforced NiCr microwave cladding on microstructure, mechanical and wear properties. J Inst Eng Ind Series D. https://doi.org/10.1007/s40033-022-00445-8
60. Nithin HS, Nishchitha KM, Pradeep DG, Durga Prasad C, Mathapati M (2023) Comparative analysis of CoCrAlY coatings at high temperature oxidation behavior using different reinforcement composition profiles. Weld World 67:585–592. https://doi.org/10.1007/s40194-022-01405-2
61. Madhusudana Reddy G, Durga Prasad C, Shetty G, Ramesh MR, Nageswara Rao T, Patil P (2022) Investigation of thermally sprayed NiCrAlY/TiO_2 and NiCrAlY/Cr_2O_3/YSZ cermet composite coatings on titanium alloys. Eng Res Exp IOP 4:025049. https://doi.org/10.1088/2631-8695/ac7946
62. Madhusudana Reddy G, Durga Prasad C, Patil P, Kakur N, Ramesh MR (2022) Elevated temperature erosion performance of plasma sprayed NiCrAlY/TiO_2 coating on MDN 420 steel substrate. Surf Topogr: Metrol Prop IOP 10:025010. https://doi.org/10.1088/2051-672X/ac6a6e
63. Madhusudana Reddy G, Durga Prasad C, Shetty G, Ramesh MR, Nageswara Rao T, Patil P (2022) High temperature oxidation behavior of plasma sprayed NiCrAlY/TiO_2 & NiCrAlY / Cr_2O_3/YSZ coatings on titanium alloy. Weld World. https://doi.org/10.1007/s40194-022-01268-7
64. Naik T, Mahantayya Mathapathi C, Prasad D, Nithin HS, Ramesh MR (2022) Effect of laser post treatment on microstructural and sliding wear behavior of HVOF sprayed NiCrC and NiCrSi coatings. Surf Rev Lett 29(1):225000. https://doi.org/10.1142/S0218625X2250007X
65. Madhusudana Reddy G, Durga Prasad C, Shetty G, Ramesh MR, Nageswara Rao T, Patil P (2021) High temperature oxidation studies of plasma sprayed NiCrAlY/TiO_2 & NiCrAlY /Cr_2O_3/YSZ cermet composite coatings on MDN-420 special steel alloy. Metallogr Microstruct Anal 10:642–651. https://doi.org/10.1007/s13632-021-00784-0
66. Madhu G, Mrityunjaya Swamy KM, Kumar DA, Durga Prasad C, Harish U (2021) Evaluation of hot corrosion behavior of HVOF thermally sprayed Cr_3C_2 -35NiCr coating on SS 304 boiler tube steel. Am Inst Phys DOI 10(1063/5):0038279
67. Prasad CD, Joladarashi S, Ramesh MR, Srinath MS (2020) Microstructure and tribological resistance of flame sprayed CoMoCrSi/WC-CrC-Ni and CoMoCrSi/WC-12Co composite coatings remelted by microwave hybrid heating. J Bio Tribo-Corrosion 6:124. https://doi.org/10.1007/s40735-020-00421-3
68. Prasad CD, Joladarashi S, Ramesh MR (2020) Comparative investigation of HVOF and flame sprayed CoMoCrSi coating. Am Inst Phys 2247:050004. https://doi.org/10.1063/5.0003883
69. Prasad CD, Jerri A, Ramesh MR (2020) Characterization and sliding wear behavior of iron based metallic coating deposited by HVOF process on low carbon steel substrate. J Bio Tribo-Corros 6:69. https://doi.org/10.1007/s40735-020-00366-7
70. Reddy MS, Durga Prasad C, Pradeep Patil MR, Ramesh NR (2021) Hot corrosion behavior of plasma sprayed NiCrAlY/TiO_2 and NiCrAlY/Cr_2O_3/YSZ cermets coatings on alloy steel. Surf Interfaces 22:100810
71. Prasad CD, Joladarashi S, Ramesh MR, Srinath MS, Channabasappa BH (2020) Comparison of high temperature wear behavior of microwave assisted HVOF sprayed CoMoCrSi-WC-CrC-Ni/WC-12Co composite coatings. SILICON 12:3027–3045. https://doi.org/10.1007/s12633-020-00398-1
72. Girisha KG, Rakesh R, Durga Prasad C, Sreenivas Rao KV (2015) Development of corrosion resistance coating for AISI 410 grade steel. Appl Mech Mater 813–814:135–139. https://doi.org/10.4028/www.scientific.net/AMM.813-814.135

73. Prasad CD, Joladarashi S, Ramesh MR, Srinath MS, Channabasappa BH (2019) Development and sliding wear behavior of Co-Mo-Cr-Si cladding through microwave heating. SILICON 11:2975–2986. https://doi.org/10.1007/s12633-019-0084-5
74. Prasad CD, Joladarashi S, Ramesh MR, Srinath MS, Channabasappa BH (2019) Microstructure and tribological behavior of flame sprayed and microwave fused CoMoCrSi/CoMoCrSi-Cr_3C_2 coatings. Mater Res Exp, IOP 6:026512. https://doi.org/10.1088/2053-1591/aaebd9
75. Girisha KG, Sreenivas Rao KV, Durga Prasad C (2018) Slurry erosion resistance of martenistic stainless steel with plasma sprayed Al2O3–40%TiO2 coatings. Mater Today Proceed 5:7388–7393. https://doi.org/10.1016/j.matpr.2017.11.409
76. Prasad CD, Joladarashi S, Ramesh MR, Srinath MS, Channabasappa BH (2018) Influence of microwave hybrid heating on the sliding wear behaviour of HVOF sprayed CoMoCrSi coating. Mater Res Exp, IOP 5:086519. https://doi.org/10.1088/2053-1591/aad44e
77. Durga Prasad C, Sharnappa Joladarashi MR, Ramesh AS (2018) High Temperature gradient cobalt based clad developed using microwave hybrid heating. Am Inst Phy 1943:020111. https://doi.org/10.1063/1.5029687
78. Girisha KG, Durga Prasad C, Anil KC, Sreenivas Rao KV (2015) Dry sliding wear behaviour of Al2O3 coatings for AISI 410 grade stainless steel. Appl Mech Mater 766–767:585–589. https://doi.org/10.4028/www.scientific.net/AMM.766-767.585
79. Fantozzi D, Matikainen V, Uusitalo M, Koivuluoto H, Vuoristo P (2017) Chlorine-induced high temperature corrosion of Inconel 625 sprayed coatings deposited with different thermal spray techniques. Surf Coat Technol 318:233–243
80. Bansal A, Goyal DK, Singh P, Singla AK, Gupta MK, Bala N, Kolte J, Setia G (2020) Erosive wear behaviour of HVOF-sprayed Ni-20Cr_2O_3 coating on pipeline materials. Int J Refract Metals Hard Mater 92:105332
81. Chen L, Lan H, Huang C, Yang B, Lingzhong Du, Zhang W (2017) Hot corrosion behavior of porous nickel-based alloys containing molybdenum in the presence of NaCl at 750° C. Eng Fail Anal 79:245–252
82. Wei B, Chen C, Jin Xu, Yang L, Jia Y, Yao Du, Guo M, Sun C, Wang Z, Wang F (2022) Comparing the hot corrosion of (100), (210) and (110) Ni-based superalloys exposed to the mixed salt of N_a2S_O4-NaCl at 750° C: Experimental study and first-principles calculation. Corros Sci 195:109996
83. Wang J, Li D, Shao T (2022) Hot corrosion and electrochemical behavior of NiCrAlY, NiCoCrAlY and NiCoCrAlYTa coatings in molten NaCl-Na_2SO_4 at 800° C. Surf Coat Technol 440:128503
84. Chen L, Zhang X, Yue Wu, Chen C, Li Y, Zhou W, Ren X (2022) Effect of surface morphology and microstructure on the hot corrosion behavior of TiC/IN625 coatings prepared by extreme high-speed laser cladding. Corros Sci 201:110271
85. Hasegawa M, Hirata K, Dlouhý I (2019) Microstructural change and fracture behavior under different heat exposure conditions on thermal barrier coatings deposited on tial intermetallic compound. Key Eng Mater 810:27–33
86. Kaplan M, Uyaner M, Ozgurluk Y, Doleker KM, Karaoglanli AC (2019) Evaluation of hot corrosion behavior of APS and HVOF sprayed thermal barrier coatings (TBCs) exposed to molten Na_2SO_4+ V_2O_5 salt at 1000 C. Eng Des Appl. https://doi.org/10.1007/978-3-319-79005-3_28
87. Wei Z, Yuping Wu, Hong S, Cheng J, Qiao L, Cheng J, Zhu S (2021) Ultrasonic cavitation erosion behaviors of high-velocity oxygen-fuel (HVOF) sprayed AlCoCrFeNi high-entropy alloy coating in different solutions. Surf Coat Technol 409:126899
88. Muthu SM, Arivarasu M, Arivazhagan N (2019) Investigation of hot corrosion resistance of bare and Ni-20% Cr coated superalloy 825 to Na_2SO_4-60% V_2O_5 environment at 900° C. Proced Struct Integr 14:290–303
89. Hao E, An Y, Zhao X, Zhou H, Chen J (2018) NiCoCrAlYTa coatings on nickel-base superalloy substrate: deposition by high velocity oxy-fuel spraying as well as investigation of mechanical properties and wear resistance in relation to heat-treatment duration. Appl Surf Sci 462:194–206
90. Somasundaram B, Navinesh BC, Jegadeeswaran N (2021) Erosion behaviour of HVOF sprayed WC. Co-NiCrAlYSi (35%-65%) coatings. Mater Today: Proceed 45:372–376
91. Ramkumar KD, Abraham WS, Viyash V, Arivazhagan N, Rabel AM (2017) Investigations on the microstructure, tensile strength and high temperature corrosion behaviour of Inconel 625 and Inconel 718 dissimilar joints. J Manuf Process 25:306–322
92. Zhang G, Sun Y, Gao H, Zuo D, Liu Xu (2021) A theoretical and experimental investigation of particle embedding and erosion behaviour of PDMS in micro-abrasive air-jet machining. Wear 486:204118
93. Chen L, Zhao Yu, Guan C, Tianbiao Yu (2021) Effects of CeO_2 addition on microstructure and properties of ceramics reinforced Fe-based coatings by laser cladding. Int J Adv Manuf Technol 115:2581–2593
94. Alok V, Kumar A, Patnaik A, Meena ML (2021) Influence of deposition parameters on tribological performance of HVOF coating: a review. Materials science and engineering. IOP Publishing, Bristol, p 012015
95. Sharma AK, Perumal G, Arora HS, Grewal HS (2021) Slurry erosion-corrosion resistance of MoNbTaTiZr high entropy alloy. J Bio-Tribo-Corros 7:1–10
96. Xu J, Peng S, Li Z, Jiang S, Xie Z-H, Munroe P, Hong Lu (2021) Remarkable cavitation erosion–corrosion resistance of CoCrFeNiTiMo high-entropy alloy coatings. Corros Sci 190:109663
97. Ozgurluk Y, Gulec A, Ozkan D, Binal G, Karaoglanli AC (2023) Structural characteristics, oxidation performance and failure mechanism of thermal barrier coatings fabricated by atmospheric plasma spraying and detonation gun spraying. Eng Fail Anal 152:107499
98. Yuan K, Zhu J, Dong W, Yueguang Yu, Xiaoliang Lu, Ji X, Wang X (2017) Applying low-pressure plasma spray (LPPS) for coatings in low-temperature SOFC. Int J Hydrogen Energy 42(34):22243–22249
99. Kumar R, Kumar R, Kumar S (2018) Erosion corrosion study of HVOF sprayed thermal sprayed coating on boiler tubes: a review. IJSMS. https://doi.org/10.51386/25815946/ijsms-v1i3p101
100. Abhijith NV, Kumar D, Kalyansundaram D (2022) Development of single-stage TiNbMoMnFe high-entropy alloy coating on 304L stainless steel using HVOF thermal spray. J Therm Spray Technol 31(4):1032–1044
101. Azizpour MJ, Tolouei-Rad M (2019) The effect of spraying temperature on the corrosion and wear behavior of HVOF thermal sprayed WC-Co coatings. Ceram Int 45(11):13934–13941
102. Silveira LL, Pukasiewicz AGM, de Aguiar DJM, Zara AJ, Björklund S (2019) Study of the corrosion and cavitation resistance of HVOF and HVAF FeCrMnSiNi and FeCrMnSiB coatings. Surf Coat Technol 374:910–922
103. Ghadami F, Sabour Rouh Aghdam A, Ghadami S (2020) Mechanism of the oxide scale formation in thermally-sprayed NiCoCrAlY coatings modified by CeO_2 nanoparticles. Mater Today Commun 24:101357
104. Upadhyaya R, Tailor S, Shrivastava S, Modi SC (2018) High performance thermal-sprayed WC-10Co-4Cr coatings in narrow and complex areas. Surf Eng 34(5):412–421
105. Anand Babu K, Jegadeeswaran N, Nithin HS, Kapilan N (2021) Studies on solid particle erosion by HVOF sprayed

25%(Cr3C2-25 (Ni20Cr))+ 75% NiCrAlY on Ti-31. Mater Today: Proceed 45:246–253
106. Ghadami F, Sabour Rouh Aghdam A, Ghadami S (2020) Isothermal and cyclic oxidation behavior of HVOF-Sprayed NiCoCrAlY coatings: comparative investigations on the conventional and nanostructured coatings. J Therm Spray Technol 29:1926–1942
107. Lynam A, Rincon Romero A, Xu F, Wellman RW, Hussain T (2022) Thermal spraying of ultra-high temperature ceramics: a review on processing routes and performance. J Therm Spray Technol 31(4):745–779
108. Chen Y, Yuping Wu, Hong S, Long W, Ji X (2020) The effect of impingement angle on erosion wear characteristics of HVOF sprayed WC-Ni and WC-Cr_3C_2-Ni cermet composite coatings. Mater Res Exp 7(2):026503
109. Thermsuk S, Surin P (2019) Optimization parameters of WC-12Co HVOF sprayed coatings on SUS 400 stainless steel. Proced Manuf 30:506–513
110. Ding X, Cheng X-D, Shi J, Li C, Yuan C-Q, Ding Z-X (2018) Influence of WC size and HVOF process on erosion wear performance of WC-10Co4Cr coatings. Int J Adv Manuf Technol 96:1615–1624
111. Matikainen V, Rubio Peregrina S, Ojala N, Koivuluoto H, Schubert J, Houdková Š, Vuoristo P (2019) Erosion wear performance of WC-10Co4Cr and Cr3C2–25NiCr coatings sprayed with high-velocity thermal spray processes. Surf Coat Technol 370:196–212
112. Qadir D, Sharif R, Nasir R, Awad A, Mannan HA (2023) A review on coatings through thermal spraying. Chem Papers. https://doi.org/10.1007/s11696-023-03089-4
113. López-Ortega A, Arana JL, Rodríguez E, Bayón R (2018) Corrosion, wear and tribocorrosion performance of a thermally sprayed aluminum coating modified by plasma electrolytic oxidation technique for offshore submerged components protection. Corros Sci 143:258–280
114. Meghwal A, Ameey Anupam BS, Murty CC, Berndt RS, Kottada AS, Ang M (2020) Thermal spray high-entropy alloy coatings: a review. J Therm Spray Technol 29:857–893
115. Zhao W, Kong D (2019) Effects of laser power on immersion corrosion and electrochemical corrosion performances of laser thermal sprayed amorphous AlFeSi coatings. Appl Surf Sci 481:161–173
116. Wood RJK, Herd S, Thakare MR (2018) A critical review of the tribocorrosion of cemented and thermal sprayed tungsten carbide. Tribol Int 119:491–509
117. Ozgurluk Y, Doleker KM, Karaoglanli AC (2018) Hot corrosion behavior of YSZ, $Gd2Zr_2O_7$ and YSZ/$Gd2Zr_2O_7$ thermal barrier coatings exposed to molten sulfate and vanadate salt. Appl Surf Sci 438:96–113
118. Guo L, Zhang C, Li M, Sun W, Zhang Z, Ye F (2017) Hot corrosion evaluation of Gd_2O_3-Yb_2O_3 co-doped Y_2O_3 stabilized ZrO_2 thermal barrier oxides exposed to Na_2SO_4+ V_2O_5 molten salt. Ceram Int 43(2):2780–2785
119. Prasad CD, Kollur S, Aprameya CR, Chandramouli TV, Jagadeesha T, Prashanth BN (2023) Investigations on tribological and microstructure characteristics of WC-12Co/FeNiCrMo composite coating by HVOF process. JOM J Miner, Metals Mater Soc (TMS). https://doi.org/10.1007/s11837-023-06242-2
120. Durga Prasad C, Kollur S, Nusrathulla M, Satheesh Babu G, Hanamantraygouda MB, Prashanth BN, Nagabhushana N (2023) Characterisation and wear behaviour of SiC reinforced FeNiCrMo composite coating by HVOF process. Trans IMF. https://doi.org/10.1080/00202967.2023.2246259
121. Sharanabasava H, Raviprakash M, Durga Prasad C, Ramesh MR, Phanibhushana MV, Vasudev H, Kumar S (2023) Microstructure, mechanical and wear properties of SiC and Mo reinforced NiCr microwave cladding. Adv Mater Process Technol. https://doi.org/10.1080/2374068X.2023.2257937
122. Madhu Sudana Reddy G, Durga Prasad C, Kollur S, Avinash Lakshmikanthan R, Suresh ACR (2023) Investigation of high temperature erosion behaviour of NiCrAlY/TiO_2 plasma coatings on titanium substrate. JOM J Miner Metals Mater Soc (TMS). https://doi.org/10.1007/s11837-023-05894-4
123. Madhusudana Reddy G, Durga Prasad C, Patil P, Kakur N, Ramesh MR (2023) High Temperature erosion performance of NiCrAlY/Cr_2O_3/YSZ plasma spray coatings. Trans IMF. https://doi.org/10.1080/00202967.2023.2208899
124. Sharanabasva H, Durga Prasad C, Ramesh MR (2023) Characterization and wear behavior of nicrmosi microwave cladding. J Mater Eng Perform. https://doi.org/10.1007/s11665-023-07998-z
125. Vishnoi M, Murtaza Q, Kumar P (2021) Effect of rare earth elements on coatings developed by thermal spraying processes (TSP)–a brief review. Mater Today: Proceed 44:4053–4058
126. Kumar S, Kumar M, Handa A (2020) Erosion corrosion behaviour and mechanical properties of wire arc sprayed Ni-Cr and Ni-Al coating on boiler steels in a real boiler environment. Mater High Temp 37(6):370–384
127. Milan Shahana S, Srinivasa Rao B, Kamaraj M (2022) High-temperature oxidation and hot corrosion of thermal spray coatings. A treatise on corrosion science, engineering and technology. Springer Nature Singapore, Singapore, pp 407–420
128. Doolabi DS, Rahimipour MR, Alizadeh M, Pouladi S, Hadavi SMM, Vaezi MR (2017) Effect of high vacuum heat treatment on microstructure and cyclic oxidation resistance of HVOF-CoNiCrAlY coatings. Vacuum 135:22–33
129. Patel SK, Singh VP, Kuriachen B (2019) Friction stir processing of alloys with secondary phase particles: an overview. Mater Manuf Process 34(13):1429–1457
130. Ludwig GA, Malfatti CF, Schroeder RM, Ferrari VZ, Muller IL (2019) WC10Co4Cr coatings deposited by HVOF on martensitic stainless steel for use in hydraulic turbines: resistance to corrosion and slurry erosion. Surf Coat Technol 377:124918
131. Mago J, Bansal S, Gupta D, Jain V (2021) Influence of microwave heating on metallurgical and mechanical properties of Ni-40Cr_3C_2 composite clads in the context of cavitation erosion resistance characteristics. Proc Inst Mech Eng C J Mech Eng Sci 235(7):1258–1276
132. Berger JE, Schulz R, Savoie S, Gallego J, Kiminami CS, Bolfarini C, Botta WJ (2017) Wear and corrosion properties of HVOF coatings from Super duplex alloy modified with addition of boron. Surf Coat Technol 309:911–919